Ultrafast variational simulation of nontrivial quantum states with long-range interactions

Wen Wei Ho,[1] Cheryne Jonay,[2] and Timothy H. Hsieh[2]
[1]*Department of Physics, Harvard University, Cambridge, Massachusetts 02138, USA*
[2]*Perimeter Institute for Theoretical Physics, Waterloo, Ontario, Canada N2L 2Y5*

(Received 8 November 2018; published 22 May 2019)

State preparation protocols ideally require as minimal operations as possible in order to be implemented in near-term, potentially noisy quantum devices. Motivated by long-range interactions (LRIs) intrinsic to many present-day experimental platforms (trapped ions, Rydberg atom arrays, etc.), we investigate the efficacy of variationally simulating nontrivial quantum states using the variational quantum-classical simulation (VQCS) protocol explored recently [W. W. Ho and T. H. Hsieh, SciPost Phys. **6**, 29 (2019)], in the presence of LRIs. We show that this approach leads to extremely efficient state preparation: for example, Greenberger-Horne-Zeilinger (GHZ) states can be prepared with $O(1)$ iterations of the protocol, and a quantum critical point of the long-range transverse-field Ising model (TFIM) can be prepared with $>99\%$ fidelity on a 100-qubit system with *only one* iteration. Furthermore, we show that VQCS with LRIs is a promising route for exploring generic points in the phase diagram of the long-range TFIM. Our approach thus provides concrete, ultrafast protocols for quantum simulators equipped with long-range interactions.

DOI: 10.1103/PhysRevA.99.052332

I. INTRODUCTION

Rapid experimental progress in the control of synthetic quantum systems, such as trapped ions [1–3], ultracold atoms [4–6], and superconducting qubits [7,8], has ushered in the era of so-called noisy intermediate-scale quantum (NISQ) technology [9], where quantum devices of up to 50–100 qubits can be coherently manipulated. This has unlocked the potential for quantum computation [8,10], quantum sensing and metrology [11–14], and also the simulation of quantum many-body phases of matter [4,15–22]. Such tasks require the ability to create, with good fidelities, quantum states containing nontrivial entanglement, such as the Greenberger-Horne-Zeilinger (GHZ) state, quantum critical states, and topologically ordered states. A central challenge is therefore finding efficient state preparation protocols that can be implemented in these noisy, imperfect quantum platforms: ideally, protocols should have as minimal a circuit depth as possible to be realistically implemented, in order to suppress the errors that accumulate during runtime.

Recently, the variational quantum-classical simulation (VQCS) protocol was proposed as one such candidate [23]. In short, the VQCS protocol is a hybrid quantum-classical bang-bang protocol which specifically incorporates feedback and is motivated by the quantum approximate optimization algorithm (QAOA) [24,25] as well as various variational quantum eigensolvers [26,27]. It works as follows: After initializing in an easily prepared state, a set of angles is fed into the quantum simulator, which specifies the durations for which time evolution between two different Hamiltonians is alternated between. Measurements are then performed to estimate the energy of the resulting state with respect to a target (generally quantum) Hamiltonian. The energy cost function is subsequently optimized on a classical computer to yield a new set of angles, and the process is iterated until the cost function is minimized. With spatially local Hamiltonians and finite evolution times, the VQCS has been shown to be able to transform trivial product states into GHZ, quantum critical, and topologically ordered states, with perfect fidelity and iteration depths that scale as $O(N)$, where N is the system's linear dimension [23]. Conceptually, the VQCS is an example of a "shortcut to adiabaticity," a direction in quantum state control that is actively being researched [28–32], as its operating principle is fundamentally different from conventional adiabatic preparation schemes [33–38].

While an iteration depth scaling as $O(N)$ is efficient from a theoretical standpoint—there exist fundamental speed limitations imposed by Lieb-Robinson bounds [39–42] constraining unitary circuits utilizing spatially local Hamiltonians—it still presents challenges experimentally, especially in terms of scalability to a large number of qubits in near-term devices. This motivates the search for alternative ultrafast protocols. A possible way to overcome these speed limitations is to utilize long-range interactions (LRIs) that are naturally present in various experimental quantum simulator platforms, e.g., trapped-ion systems (Coulomb interactions) and Rydberg atom arrays (van der Waals interactions) [2,6,43]. With LRIs, entanglement and correlations can be built up between distant parts of the system in finite time [44–46], potentially (though not obviously) allowing for a quick preparation of desired long-range correlated states.

To this end, in this work we explore how efficiently the VQCS protocol with long-range interactions can prepare nontrivial quantum states. Specifically, we consider in mind quantum simulators (digital or analog) that realize long-range $\sim 1/r^{\alpha}$ Ising interactions with tunable range α, motivated in large part by trapped-ion experimental setups. We find that the VQCS protocol with LRIs can prepare GHZ and quantum critical states with $O(1)$ iterations. In particular, in the limit of extremely long-range interactions, the GHZ state

can be prepared with only one (two) iteration(s) for odd (even) system sizes. Furthermore, the quantum critical point (QCP) of the Lipkin-Meshkov-Glick model [47] can be prepared with high fidelity very quickly (e.g., fidelity >0.99 for 100 spins after one iteration). We also analyze how efficiently the protocol can prepare points within the phase diagram of the long-range transverse-field Ising model. Our results thus demonstrate the utility of VQCS protocols with LRIs for near-term, potentially noisy quantum simulators to realize nontrivial many-body states of interest.

II. VQCS PROTOCOL

We quickly recapitulate the VQCS protocol [23]. Our aim is to prepare a target state $|\psi_t\rangle$ with as high a fidelity as possible, given resources available in a quantum simulator (either digital or analog) such as single qubit rotations and interactions between qubits, which we denote schematically by H_1, H_2. Usually, $|\psi_t\rangle$ will be taken to be the ground state of some target Hamiltonian H_t which is a linear combination of H_1, H_2. Henceforth, in this work we take $H_1 = -\sum_i X_i$, a global transverse field, but this can be relaxed.

The VQCS starts off with an easily prepared initial state, such as the unentangled ground state $|+\rangle$ of the paramagnet H_1. One then time evolves in an alternating fashion between H_1 and the "interaction Hamiltonian" H_2, for a total of p iterations:

$$|\psi(\vec{\gamma},\vec{\beta})\rangle_p = e^{-i\beta_p H_1} e^{-i\gamma_p H_2} \cdots e^{-i\beta_1 H_1} e^{-i\gamma_1 H_2} |+\rangle, \quad (1)$$

with evolution times given by angles $(\vec{\gamma},\vec{\beta}) \equiv (\gamma_1, \cdots, \gamma_p, \beta_1, \cdots, \beta_p)$. We label this protocol as VQCS$_p$.

As the goal is to closely approximate H_t's ground state, one can seek to find the evolution times $(\vec{\gamma},\vec{\beta})$ which minimize a given cost function $F_p(\vec{\gamma},\vec{\beta})$, usually taken to be the energy with respect to the target Hamiltonian H_t:

$$F_p(\vec{\gamma},\vec{\beta}) = {}_p\langle\psi(\vec{\gamma},\vec{\beta})|H_t|\psi(\vec{\gamma},\vec{\beta})\rangle_p. \quad (2)$$

Obviously, increasing p can only improve the minimal value F_p^*, i.e., $F_{p+1}^* \leqslant F_p^*$.

In practice, such a protocol can be implemented in a hybrid setup involving a quantum simulator and a classical computer: one first feeds the quantum simulator an initial seed of angles, producing a state $|\psi(\vec{\gamma},\vec{\beta})\rangle$. Then, leveraging upon the single-site accessibility possible in many present-day quantum simulators, one measures correlations within the state and determines the cost function (2), e.g., the global energy. A classical computer is then used to obtain the next set of angles $(\vec{\gamma},\vec{\beta})$ to be fed into the quantum simulator, by means of an optimization algorithm such as gradient descent or a similar protocol. The entire process is then repeated until either the global minimum F_p^* is found, or a desired energy or fidelity threshold is attained. As a matter of principle, the VQCS protocol is guaranteed to work in the limit of $p \to \infty$ for any finite size system (there always exists a finite gap), as an asymptotically slow adiabatic preparation scheme can always be trotterized to the form (1). However, nontrivial behavior and an improvement over adiabaticity can arise for small p, the regime of practical interest for experimental systems.

As an example, consider preparing the ground state of the one-dimensional nearest-neighbor transverse-field Ising model (TFIM), a situation considered in Ref. [23]:

$$H_{\mathrm{TFIM}} = -\sum_{i=1}^{N} Z_i Z_{i+1} - h\sum_{i=1}^{N} X_i, \quad (3)$$

where h parametrizes the field strength and N is the number of qubits. Given this H_t, a natural choice is $H_2 = -\sum_{i=1}^{N} Z_i Z_{i+1}$, which are interactions (approximately) naturally realizable in, e.g., trapped ions or Rydberg array simulators. Indeed, in a previous work, it was shown that such a VQCS$_{p^*}$ at $p^* = N/2$ can target with *perfect fidelity* the ground states of the model at $h = 0, 1$ (GHZ and quantum critical state, respectively) [23]. It was further conjectured and supported with numerical evidence that this result generalizes to all points $h \in \mathbb{R}$.

III. VQCS WITH LONG-RANGE INTERACTIONS

Despite impressive progress in the coherent control and manipulation of quantum systems today, such platforms are inherently noisy, and so it is desirable to have state preparation protocols that require as few iterations and as short a runtime as possible. However, there fundamentally exist speed limits (specifically, Lieb-Robinson bounds) in systems with local interactions to create a desired quantum state containing long-range entanglement—the time taken is $t \geqslant O(N)$ (as illustrated explicitly in the example above). Intuitively, this arises from the linear light cone $r \sim vt$ of information propagation that limits the speed at which spatially distant regions entangle.

LRIs have less stringent speed limits [46] and can potentially dramatically speed up state preparation protocols. We now show in the rest of the paper that the VQCS (1) with LRIs is a viable method for efficiently targeting nontrivial quantum states. We consider quantum simulators where long-range Ising interactions $H_2 = -\sum_{i<j}^{N} J_{ij} Z_i Z_j$ with $J_{ij} = \frac{J_0}{|i-j|^\alpha}$ for some power-law exponent α can be realized, such as trapped-ion setups or Rydberg atom array setups. Concretely, together with a readily applicable transverse field H_1, we study the following prototypical, realizable effective Hamiltonians:

$$H_t = -\sum_{i<j}^{N} J_{ij} Z_i Z_j - \mathcal{N} h \sum_{i}^{N} X_i. \quad (4)$$

In trapped-ion setups, α can vary in principle between 0 and 3, with experiments having been conducted using α ranging from 0.67 to 1.05 [3], while in Rydberg atom array setups, $\alpha = 6$. We have chosen $J_0 = 1$ and normalized (4) in a standard way [2] so that $\mathcal{N} = \frac{1}{N-1}\sum_{i<j} J_{ij}$. Note that $\alpha \to \infty$ reduces to the nearest-neighbor TFIM model with open boundary conditions.

IV. ULTRAFAST STATE PREPARATION USING VQCS WITH LONG-RANGE INTERACTIONS

We now analyze the small-α regime of Hamiltonian (4) and show that VQCS protocols (1) using H_1, H_2 as defined above, with $p = O(1)$, are sufficient to prepare certain target ground states. We restrict the VQCS parameter space to

$\gamma_i \in [-\pi, \pi)$ and $\beta_i \in [0, \pi/2)$. The former is motivated by experimental limitations on the evolution time, and the latter is because $e^{-i(\pi/2)H_X} \propto \prod_i X_i$ which is conserved throughout the evolution.

A. GHZ state preparation, $\alpha = 0$

First consider the case $\alpha = 0$ of (4), in which the N qubits interact in an all-to-all fashion. Then, up to an overall multiplicative factor and also an inconsequential shift in energy, (4) is equivalent to the Lipkin-Meshkov-Glick (LMG) model

$$H_{\mathrm{LMG}} = -\frac{2}{N} S_z^2 - 2gS_x, \tag{5}$$

where the total spin operators are $S_z = \sum_i^N Z_i/2$ and $S_x = \sum_i^N X_i/2$, and $g = h/2$. As is the case with the nearest-neighbor TFIM, its ground states are ferromagnetic GHZ states at $g = 0$, and a quantum phase transition at $g = 1$ separates the ferromagnet from the paramagnetic phase.

We claim a $p = O(1)$ VQCS circuit suffices to produce the ground state of (5) at $g = 0$, i.e., the GHZ state. To see this, we explicitly derive the energy cost function (2) for the LMG model with VQCS$_{p=1}$:

$$\begin{aligned} F_{p=1}(\gamma, \beta) = &-\frac{N-1}{4}(\sin(2\beta)^2(1-\cos(4\gamma)^{N-2}) \\ &+ 2\sin(4\beta)\sin(2\gamma)\cos(2\gamma)^{N-2}) \\ &- gN\cos(2\gamma)^{N-1} - 1/2 \end{aligned} \tag{6}$$

(see Appendix A for the derivation). From the above, it is evident that for odd N, the ground-state energy of $H_{\mathrm{LMG}}|_{g=0}$, namely, $E_0 = -N/2$, can be achieved with angles $(\gamma, \beta) = (\pi/4, \pi/4)$. In other words, the ferromagnetic GHZ state, a state with macroscopic superposition of entanglement $(1/\sqrt{2})(|0\cdots0\rangle + |1\cdots1\rangle)$, can be created with just two operations:

$$|\mathrm{GHZ}\rangle = e^{-i(\pi/4)H_X} e^{-i(\pi/4)H_I} |+\rangle. \tag{7}$$

We note that there exist various preparation schemes that create macroscopic GHZ states, one of which is the Molmer-Sorenson (MS) protocol involving time evolution with S_x^2 [48,49]. Although the VQCS protocol discussed above somewhat resembles the MS protocol, there are several differences: MS begins with the (Ising-symmetry-broken) ground state $|0\cdots0\rangle$ and, for odd system sizes, involves time evolution with S_x^2 and S_x, to produce a GHZ state with a relative phase between the Schrödinger cat states. A single qubit gate, or alternatively time evolution with S_z, can remove the relative phase.

The distinction between MS and our protocol is most manifest for even system sizes, in which we find that the GHZ state is instead achieved with perfect fidelity with a $p = 2$ VQCS protocol:

$$|\mathrm{GHZ}\rangle = e^{-i(\pi/4)H_X} e^{-i(\pi/8)H_I} e^{-i(3\pi/4N)H_X} e^{-i(\pi/4)H_I} |+\rangle.$$

Note that from (6), there is no range of parameters that give perfect fidelity for $p = 1$ for even N. We show in Appendix B the derivation of the above result. These results already demonstrate the utility of VQCS with LRIs: they enable ultrafast preparation of a macroscopic GHZ state, with perfect fidelity.

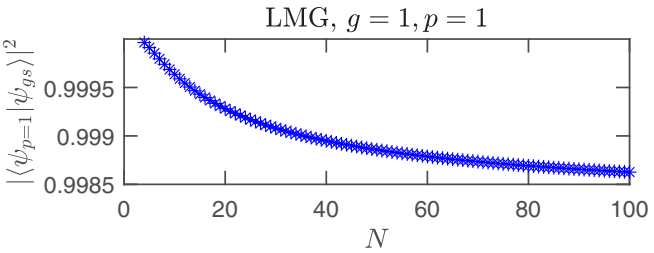

FIG. 1. Fidelity $|\langle\psi_{QCP}|\psi(\vec{\gamma}, \vec{\beta})\rangle_{p=1}|^2$ in preparation of LMG critical state as a function of system size N, for VQCS depth $p = 1$. Remarkably, even at $N = 100$, the fidelity is very close to unity (>99%).

B. Quantum critical state preparation, $\alpha = 0$

Besides the GHZ state, we find the approach can target many other interesting states. One state of particular interest is the quantum critical point of the LMG model at $g = 1$, a highly correlated state $|\psi_{QCP}\rangle$. By numerically optimizing for the energy of (5) at $g = 1$, we find that the $p = 1$ VQCS protocol is already sufficient to achieve the critical state with extremely high fidelity, $|\langle\psi_{QCP}|\psi(\vec{\gamma}, \vec{\beta})\rangle_{p=1}|^2$, even for very large system sizes (>99% at ∼100 qubits) (see Fig. 1). This is a remarkably efficient protocol for preparing a critical state.

Note that the gap at the critical point of the LMG model scales as $\Delta \propto N^{-1/3}$ [47], and thus the adiabatic algorithm requires $O(N^{1/3})$ time to prepare the GHZ and critical states. However, in order to make a meaningful comparison of the VQCS with the adiabatic algorithm, we would need to scale down the exchange interaction in (5) (i.e., J_0) by N, and thus the total preparation time for the VQCS protocol in this convention would go as N. Our intention is not to make this theoretical comparison, but instead to make contact with existing experiments. In the trapped-ion setups of Ref. [2], the nearest-neighbor exchange interaction J_0 does not necessarily decrease with system size; for example, it is (0.82, 0.56, 0.38, 0.65) kHz for $N = (8, 12, 16, 53)$, respectively. Hence, the interactions in (5) are reasonable in near-term trapped-ion experiments and lead to $O(1)$ preparation time for the GHZ and critical states. The simplicity and discreteness of the protocols we have presented may offer advantages over

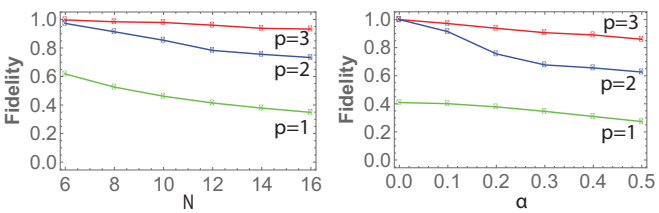

FIG. 2. Left: Fidelity in preparation of GHZ state as a function of system size N, for $\alpha = 0.2$. The fidelity decreases with increasing N; however, this can be compensated by going to higher ps. Right: Fidelity in preparation of GHZ state as a function of α, for $N = 14$.

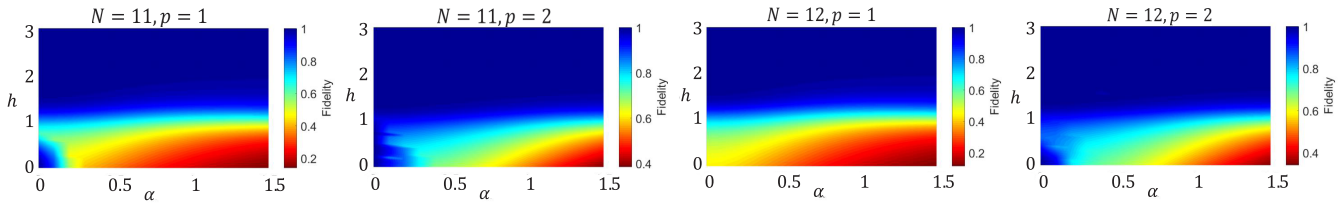

FIG. 3. Heat map depicting fidelities in the state preparation of the ground state of the long-range TFIM [Eq. (3)] for system sizes $N = 11$ and 12, for $p = 1, 2$. Blue (red) demarcates regions of high (low) fidelity. As noted before, there is an odd-even system size distinction near $\alpha \approx 0$, $h \approx 0$ for $p = 1$, but this distinction vanishes at the next level, $p = 2$.

the adiabatic algorithm with or without counterdiabatic terms [32,50–52].

C. GHZ preparation with finite α

In practice, there may be challenges in realizing strictly all-to-all ($\alpha = 0$) Ising interactions, and therefore we analyze how well a finite-α VQCS protocol can prepare the GHZ state.

In the left panel of Fig. 2, we fix $\alpha = 0.2$ and show the fidelity with the GHZ state achieved for $\text{VQCS}_{p=1,2,3}$ for even system sizes. As expected, $\text{VQCS}_{p=2}$ no longer prepares the state with perfect fidelity unlike the $\alpha = 0$ case, but this can be addressed with further iterations of VQCS. In particular, note the high fidelities achieved by $p = 3$ for system sizes up to $N = 16$. As LRIs establish correlations between spins separated by a distance r in time $O(r^{\alpha})$, which surpasses the light-cone bound for local interactions [44–46], we expect that the depth required to prepare the state with some fixed error in fidelity scales as $O(N^{\alpha'})$, $\alpha' < 1$. Also plotted is the optimal fidelity for different values of α and for fixed system size $N = 14$; the results indicate that longer-range interactions (smaller α) tend to be more effective in targeting the desired state, and that errors can be effectively reduced using further VQCS iterations [53].

D. Phase diagram of the long-range TFIM

Finally, we explore how well the VQCS protocol with LRIs can prepare the ground states at generic points in the phase diagram of the long-range TFIM model (4). It is known that the long-range TFIM supports a ferromagnetic-paramagnetic ground-state quantum phase transition for any value of α, upon tuning h. In the limit $\alpha \to 0$, the critical field $h_c = 2$, while in the limit $\alpha \to \infty$, the critical field $h_c = 1$. For intermediate values of α, previous works have attempted to map out how h_c varies (see, e.g., Refs. [54,55], and Refs. [56,57] for the antiferromagnetic model).

Plotted in Fig. 3 are the fidelities obtained from VQCS as a function of transverse field h and interaction range α, for $N = 11, 12$ and for $p = 1, 2$. As expected, at the system sizes considered, the VQCS with LRIs is able to target ground states within the paramagnetic phase (large h) relatively easily, while for the ferromagnetic phase (small h) it becomes more difficult to prepare, especially as the interactions become more short ranged (larger α). Note that for large α, the region where state preparation is difficult (red region) is separated from the region where state preparation is easy (blue region) by $h \approx 1$, which agrees with the critical point h_c of the nearest-neighbor TFIM, which is realized in the asymptotic limit $\alpha \to \infty$.

As the small-α regime of this model is somewhat challenging for numerical studies [54], it serves as a venue in which the quantum-classical hybrid implementation of VQCS could provide valuable input. Moreover, the small-α window is precisely the regime in which the VQCS approach requires only a few iterations.

V. DISCUSSION AND CONCLUSION

We have shown that VQCS-type protocols with long-range interactions allow for ultrafast state preparation. In particular, the Ising-symmetric GHZ state can be prepared exactly at finite depth $p = 1$ (2) for odd (even) system sizes. We have also demonstrated that other states of interest, for example, the quantum critical point of the Lipkin-Meshkov-Glick model, can also be prepared very efficiently. More broadly, since the VQCS protocol is very general and not only restricted to the states considered [see Eq. (1)], our results suggest that VQCS with LRIs is a promising and viable state preparation protocol that can be utilized to target other nontrivial states of interest, potentially also allowing for their efficient preparation.

VQCS with long-range interactions thus provides an opportunity for near-term simulators to prepare nontrivial states with very high fidelity, and to shed light on areas of phase diagrams that are challenging for numerics. The simplicity and efficiency of the protocols make them particularly well suited for near-term quantum devices endowed with long-range interactions, such as trapped-ion or Rydberg atom arrays.

Note added. Recently, we became aware of related, variational state preparation works [58,59].

ACKNOWLEDGMENTS

We thank R. Islam, C. Monroe, and B. Yoshida for useful discussions. W.W.H. is supported by the Gordon and Betty Moore Foundation's EPiQS Initiative through Grant No. GBMF4306. Research at Perimeter Institute is supported by the Government of Canada through Industry Canada and by the Province of Ontario through the Ministry of Research and Innovation. This work was performed in part at the Aspen Center for Physics, which is supported by National Science Foundation Grant No. PHY-1607611.

APPENDIX A: LMG COST FUNCTION FOR $p = 1$

We evaluate

$$\langle +|e^{i\gamma H_I} e^{i\beta H_X} H_{\mathrm{LMG}} e^{-i\beta H_X} e^{-i\gamma H_I}|+\rangle, \tag{A1}$$

where

$$H_{\mathrm{LMG}} = -\frac{2}{N} S_z^2 - 2gS_x. \tag{A2}$$

The second piece gives

$$-g\langle +|e^{i\gamma H_I} \sum_i X_i e^{-i\gamma H_I}|+\rangle \tag{A3}$$

$$= -g\langle +|\prod_{j\neq i}(\cos(\gamma) - i\sin(\gamma) Z_i Z_j) \sum_i X_i \prod_{j\neq i}(\cos(\gamma) + i\sin(\gamma) Z_i Z_j)|+\rangle. \tag{A4}$$

Because any operator aside from identity and X has zero expectation value in $|+\rangle$, we get contributions only from $\cos^2(\gamma) - \sin^2(\gamma)$ for each j. In total, this piece is $(-gN)(\cos(2\gamma))^{N-1}$.

The first piece is

$$-\frac{N-1}{2}\langle +|e^{i\gamma H_I} e^{i\beta H_X} Z_i Z_j e^{-i\beta H_X} e^{-i\gamma H_I}|+\rangle - \frac{1}{2} \tag{A5}$$

$$= -\frac{N-1}{2}\langle +|e^{i\gamma H_I}(\cos(2\beta) Z_i - \sin(2\beta) Y_i)(\cos(2\beta) Z_j - \sin(2\beta) Y_j) e^{-i\gamma H_I}|+\rangle - \frac{1}{2}. \tag{A6}$$

Again, we need only consider when the identity and X operators arise. One contribution to the matrix element comes from the evolution of $Y_i Z_j + Z_i Y_j$, which gives

$$-\sin(4\beta)\langle +|\prod_{k\neq j,i}(\cos(\gamma) - i\sin(\gamma) Z_i Z_k)(\cos(\gamma) - i\sin(\gamma) Z_i Z_j) \tag{A7}$$

$$\times (Y_i Z_j)(\cos(\gamma) + i\sin(\gamma) Z_i Z_j) \prod_{k\neq j,i}(\cos(\gamma) + i\sin(\gamma) Z_i Z_k)|+\rangle \tag{A8}$$

$$= \sin(4\beta)\sin(2\gamma)\cos(2\gamma)^{N-2}. \tag{A9}$$

Another contribution comes from

$$\sin(2\beta)^2\langle +|\prod_{k\neq i,j}(\cos(\gamma) - i\sin(\gamma) Z_i Z_k) \prod_{l\neq i,j}(\cos(\gamma) - i\sin(\gamma) Z_j Z_l) Y_i Y_j \tag{A10}$$

$$\times \prod_{k\neq i,j}(\cos(\gamma) + i\sin(\gamma) Z_i Z_k) \prod_{l\neq i,j}(\cos(\gamma) + i\sin(\gamma) Z_j Z_l)|+\rangle. \tag{A11}$$

The transformation into two X operators requires an odd number of applications of $Z_i Z_k$ and $Z_j Z_k$; each application comes with a factor of $\sin(2\gamma)^2$. The terms which do not alter the operator come with factors of $\cos(2\gamma)^2$. Hence, to single out the odd powers, we take the combination

$$(1/2)((\cos(2\gamma)^2 + \sin(2\gamma)^2)^{N-2} - (\cos(2\gamma)^2 - \sin(2\gamma)^2)^{N-2}) \tag{A12}$$

$$= (1/2)(1 - \cos(4\gamma)^{N-2}). \tag{A13}$$

In total, the cost function is thus

$$-\frac{N-1}{4}(\sin(2\beta)^2(1 - \cos(4\gamma)^{N-2}) + 2\sin(4\beta)\sin(2\gamma)\cos(2\gamma)^{N-2}) - gN(\cos(2\gamma))^{N-1} - 1/2. \tag{A14}$$

APPENDIX B: GHZ PREPARATION FOR EVEN N

We show below that for an even number N of qubits,

$$|\mathrm{GHZ}\rangle = \exp\left(\frac{i\pi}{4}\sum_i X_i\right)\exp\left(\frac{i\pi}{8}\sum_{ij} Z_i Z_j\right)\exp\left(\frac{3i\pi}{4N}\sum_i X_i\right)\exp\left(\frac{i\pi}{4}\sum_{ij} Z_i Z_j\right)|+\cdots+\rangle. \tag{B1}$$

It is sufficient to establish

$$\langle\uparrow\cdots\uparrow|\exp\left(\frac{i\pi}{4}\sum_i X_i\right)\exp\left(\frac{i\pi}{8}\sum_{ij} Z_iZ_j\right)\exp\left(\frac{3i\pi}{4N}\sum_i X_i\right)\exp\left(\frac{i\pi}{4}\sum_{ij} Z_iZ_j\right)|+\cdots+\rangle=\frac{1}{\sqrt{2}}, \tag{B2}$$

up to a phase. (The Ising symmetry operator is conserved as $\prod X = 1$, so the matrix element for $\langle\downarrow\cdots\downarrow|$ will also be $\frac{1}{\sqrt{2}}$. The state $|\uparrow\rangle$ is such that $Z_i|\uparrow\rangle_i = +|\uparrow\rangle_i$ and so $|\uparrow\cdots\uparrow\rangle = \prod_i |\uparrow\rangle_i$.)

We break the matrix element in half and first evaluate the left-hand side. First,

$$\exp\left(\frac{-i\pi}{4}\sum_i X_i\right)|\uparrow\cdots\uparrow\rangle=\frac{1}{\sqrt{2^N}}\left(\prod_i(1-iX_i)\right)|\uparrow\cdots\uparrow\rangle \tag{B3}$$

$$=\frac{1}{\sqrt{2^N}}\sum_s(-i)^{(N-\sum_i z_i)/2}|z\rangle, \tag{B4}$$

where $z = \{z_1, \ldots, z_N\}$ labels a spin configuration.

Applying $\exp(\frac{-i\pi}{8}\sum_{ij} Z_iZ_j)$ and neglecting the overall phase then gives

$$\frac{1}{\sqrt{2^N}}\sum_z\exp\left(-i\pi/8\sum_{ij} z_iz_j\right)i^{\sum_i z_i/2}|z\rangle \tag{B5}$$

$$=\frac{1}{\sqrt{2^N}}\sum_z\exp\left(\frac{i\pi}{16}\big(-z_t^2+4z_t\big)\right)|z\rangle, \tag{B6}$$

where we have defined $z_t \equiv \sum_i z_i$.

The right-hand side is

$$\exp\left(\frac{3i\pi}{4N}\sum_i X_i\right)\exp\left(\frac{i\pi}{4}\sum_{ij} Z_iZ_j\right)|+\cdots+\rangle \tag{B7}$$

$$=\frac{1}{\sqrt{2^N}}\exp\left(\frac{3i\pi}{4N}\sum_i X_i\right)\sum_z\exp\left(\frac{i\pi}{4}\sum_{ij} z_iz_j\right)|z\rangle \tag{B8}$$

$$=\frac{1}{\sqrt{2^N}}\prod_i(c+isX_i)\sum_z\exp\left(\frac{i\pi}{4}\sum_{ij} z_iz_j\right)|z\rangle, \tag{B9}$$

where $c \equiv \cos(3\pi/4N)$, $s \equiv \sin(3\pi/4N)$.

Consider the contributions to the coefficient of a given spin configuration $|z\rangle$. Each contribution involves partitioning the N spins into two sets A and B of sizes a and $N-a$, respectively, and flipping the spins in set A. The resulting coefficient from this given flip is

$$c^{N-a}(is)^a\exp\left(\frac{i\pi}{4}\sum_{ij} z_iz_j\right)\exp\left(\frac{i\pi}{4}\sum_{i\in A,\,j\in B}(\bar{z}_i-z_i)z_j\right), \tag{B10}$$

where $\bar{z}_i \equiv -z_i$.

We now show that this factor only depends on the parity of a (and the particular configuration z) and, once this is fixed, the factor is independent of the partition. The final phase factor above can be written as

$$\exp\left(\frac{-i\pi}{2}z_A(z_t-z_A)\right), \tag{B11}$$

where $z_A \equiv \sum_{i\in A} z_i$. Because N is even, z_t is even. If a is even, the z_a is even and thus the phase factor is 1. Moreover, it is straightforward to check that either changing the partition (keeping partition size fixed) or changing the partition size by 2 does not change the above phase. Hence, the case of a odd can be reduced to choosing A to be the first spin. The wave function

becomes

$$\frac{1}{\sqrt{2^N}}\sum_z \exp\left(\frac{i\pi}{4}\sum_{ij} z_i z_j\right)\left(\sum_{\text{even } a}\binom{N}{a}c^{N-a}(is)^a + \sum_{\text{odd } a}\binom{N}{a}c^{N-a}(is)^a \exp\left(\frac{-i\pi}{2}z_1(z_t - z_1)\right)\right)|z\rangle$$

$$= \frac{1}{\sqrt{2^N}}\sum_z \exp\left(\frac{i\pi}{4}\sum_{ij} z_i z_j\right)\left(\cos(3\pi/4) + i\sin(3\pi/4)\exp\left(\frac{-i\pi}{2}z_1(z_t - z_1)\right)\right)|z\rangle.$$

Dropping overall phases, we get

$$\frac{1}{\sqrt{2^{N+1}}}\sum_z \exp\left(\frac{i\pi}{8}z_t^2\right)\left(1 - i\exp\left(\frac{-i\pi}{2}z_1(z_t - z_1)\right)\right)|z\rangle. \tag{B12}$$

The matrix element between left- and right-hand sides is thus

$$\frac{1}{2^N\sqrt{2}}\sum_z \exp\left(\frac{i\pi}{16}(3z_t^2 - 4z_t)\right)\left(1 - i\exp\left(\frac{-i\pi}{2}z_1(z_t - z_1\right)\right). \tag{B13}$$

Due to the last piece, any configuration with $z_t \equiv 2(\text{mod } 4)$ does not contribute and the matrix element reduces to

$$\frac{1}{2^N\sqrt{2}}\sum_{z|z_t\equiv 0(\text{mod } 4)} 2\exp\left(\frac{i\pi}{16}(3z_t^2 - 4z_t)\right) = \frac{1}{\sqrt{2}}. \tag{B14}$$

[1] R. Blatt and C. F. Roos, Quantum simulations with trapped ions, Nat. Phys. **8**, 277 (2012).

[2] J. Zhang, G. Pagano, P. W. Hess, A. Kyprianidis, P. Becker, H. Kaplan, A. V. Gorshkov, Z.-X. Gong, and C. Monroe, Observation of a many-body dynamical phase transition with a 53-qubit quantum simulator, Nature (London) **551**, 601 (2017).

[3] R. Islam, C. Senko, W. C. Campbell, S. Korenblit, J. Smith, A. Lee, E. E. Edwards, C.-C. J. Wang, J. K. Freericks, and C. Monroe, Emergence and frustration of magnetism with variable-range interactions in a quantum simulator, Science **340**, 583 (2013).

[4] M. Greiner, O. Mandel, T. Esslinger, T. W. Hänsch, and I. Bloch, Quantum phase transition from a superfluid to a Mott insulator in a gas of ultracold atoms, Nature (London) **415**, 39 (2002).

[5] I. Bloch, J. Dalibard, and W. Zwerger, Many-body physics with ultracold gases, Rev. Mod. Phys. **80**, 885 (2008).

[6] H. Bernien, S. Schwartz, A. Keesling, H. Levine, A. Omran, H. Pichler, S. Choi, A. S. Zibrov, M. Endres, M. Greiner, V. Vuletic, and M. D. Lukin, Probing many-body dynamics on a 51-atom quantum simulator, Nature (London) **551**, 579 (2017).

[7] M. H. Devoret and R. J. Schoelkopf, Superconducting circuits for quantum information: An outlook, Science **339**, 1169 (2013).

[8] J. M. Gambetta, J. M. Chow, and M. Steffen, Building logical qubits in a superconducting quantum computing system, npj Quantum Inf. **3**, 2 (2017).

[9] J. Preskill, Quantum computing in the NISQ era and beyond, Quantum **2**, 79 (2018).

[10] M. Schreiber, S. S. Hodgman, P. Bordia, H. P. Lüschen, M. H. Fischer, R. Vosk, E. Altman, U. Schneider, and I. Bloch, Observation of many-body localization of interacting fermions in a quasirandom optical lattice, Science **349**, 842 (2015).

[11] D. Leibfried, M. D. Barrett, T. Schaetz, J. Britton, J. Chiaverini, W. M. Itano, J. D. Jost, C. Langer, and D. J. Wineland, Toward Heisenberg-limited spectroscopy with multiparticle entangled states, Science **304**, 1476 (2004).

[12] V. Giovannetti, S. Lloyd, and L. Maccone, Quantum-enhanced measurements: Beating the standard quantum limit, Science **306**, 1330 (2004).

[13] C. L. Degen, F. Reinhard, and P. Cappellaro, Quantum sensing, Rev. Mod. Phys. **89**, 035002 (2017).

[14] S. Choi, N. Y. Yao, and M. D. Lukin, Quantum metrology based on strongly correlated matter, arXiv:1801.00042.

[15] M. Aidelsburger, M. Atala, M. Lohse, J. T. Barreiro, B. Paredes, and I. Bloch, Realization of the Hofstadter Hamiltonian with Ultracold Atoms in Optical Lattices, Phys. Rev. Lett. **111**, 185301 (2013).

[16] M. Aidelsburger, M. Lohse, C. Schweizer, M. Atala, J. T. Barreiro, S. Nascimbène, N. R. Cooper, I. Bloch, and N. Goldman, Measuring the Chern number of Hofstadter bands with ultracold bosonic atoms, Nat. Phys. **11**, 162 (2014).

[17] R. Islam, R. Ma, P. M. Preiss, M. Eric Tai, A. Lukin, M. Rispoli, and M. Greiner, Measuring entanglement entropy in a quantum many-body system, Nature (London) **528**, 77 (2015).

[18] J.-Y. Choi, S. Hild, J. Zeiher, P. Schauß, A. Rubio-Abadal, T. Yefsah, V. Khemani, D. A. Huse, I. Bloch, and C. Gross, Exploring the many-body localization transition in two dimensions, Science **352**, 1547 (2016).

[19] J. Smith, A. Lee, P. Richerme, B. Neyenhuis, P. W. Hess, P. Hauke, M. Heyl, D. A. Huse, and C. Monroe, Many-body localization in a quantum simulator with programmable random disorder, Nat. Phys. **12**, 907 (2016).

[20] S. Choi, J. Choi, R. Landig, G. Kucsko, H. Zhou, J. Isoya, F. Jelezko, S. Onoda, H. Sumiya, V. Khemani, C. von Keyserlingk, N. Y. Yao, E. Demler, and M. D. Lukin, Observation of discrete time-crystalline order in a disordered dipolar many-body system, Nature (London) **543**, 221 (2017).

[21] J. Zhang, P. W. Hess, A. Kyprianidis, P. Becker, A. Lee, J. Smith, G. Pagano, I.-D. Potirniche, A. C. Potter, A. Vishwanath, N. Y. Yao, and C. Monroe, Observation of a discrete time crystal, Nature (London) **543**, 217 (2017).

[22] J. Choi, H. Zhou, S. Choi, R. Landig, W. W. Ho, J. Isoya, F. Jelezko, S. Onoda, H. Sumiya, D. A. Abanin, and M. D. Lukin, Probing Quantum Thermalization of a Disordered Dipolar Spin Ensemble with Discrete Time-Crystalline Order, Phys. Rev. Lett. **122**, 043603 (2019).

[23] W. W. Ho and T. H. Hsieh, Efficient variational simulation of non-trivial quantum states, SciPost Phys. **6**, 29 (2019).

[24] E. Farhi, J. Goldstone, and S. Gutmann, A quantum approximate optimization algorithm, arXiv:1411.4028.

[25] E. Farhi and A. W. Harrow, Quantum supremacy through the quantum approximate optimization algorithm, arXiv:1602.07674.

[26] D. Wecker, M. B. Hastings, and M. Troyer, Progress towards practical quantum variational algorithms, Phys. Rev. A **92**, 042303 (2015).

[27] A. Peruzzo, J. McClean, P. Shadbolt, M.-H. Yung, X.-Q. Zhou, P. J. Love, A. Aspuru-Guzik, and J. L. O'Brien, A variational eigenvalue solver on a photonic quantum processor, Nat. Commun. **5**, 4213 (2014).

[28] M. Demirplak and S. A. Rice, Adiabatic population transfer with control fields, J. Phys. Chem. A **107**, 9937 (2003).

[29] M. Demirplak and S. A. Rice, Assisted adiabatic passage revisited, J. Phys. Chem. B **109**, 6838 (2005).

[30] M V Berry, Transitionless quantum driving, J. Phys. A **42**, 365303 (2009).

[31] K. Agarwal, R. N. Bhatt, and S. L. Sondhi, Fast Preparation of Critical Ground States Using Superluminal Fronts, Phys. Rev. Lett. **120**, 210604 (2018).

[32] D. Sels and A. Polkovnikov, Minimizing irreversible losses in quantum systems by local counterdiabatic driving, Proc. Natl. Acad. Sci. USA **114**, E3909 (2017).

[33] E. Farhi, J. Goldstone, S. Gutmann, and M. Sipser, Quantum computation by adiabatic evolution, arXiv:quant-ph/0001106.

[34] E. Farhi, J. Goldstone, S. Gutmann, J. Lapan, A. Lundgren, and D. Preda, A quantum adiabatic evolution algorithm applied to random instances of an NP-complete problem, Science **292**, 472 (2001).

[35] L. S. Pontryagin, *Mathematical Theory of Optimal Processes* (Gordon and Breach, Montreux, Switzerland, 1987).

[36] R. F. Stengel, *Optimal Control and Estimation* (Dover Publication Inc., New York, 1994).

[37] C. Brif, M. D. Grace, M. Sarovar, and K. C. Young, Exploring adiabatic quantum trajectories via optimal control, New J. Phys. **16**, 065013 (2014).

[38] Z.-C. Yang, A. Rahmani, A. Shabani, H. Neven, and C. Chamon, Optimizing Variational Quantum Algorithms Using Pontryagin's Minimum Principle, Phys. Rev. X **7**, 021027 (2017).

[39] E. H. Lieb and D. W. Robinson, The finite group velocity of quantum spin systems, Commun. Math. Phys. **28**, 251 (1972).

[40] M. A. Nielsen, A geometric approach to quantum circuit lower bounds, Quantum Info. Comput. **6**, 213 (2006), arXiv:quant-ph/0502070.

[41] S. Bravyi, M. B. Hastings, and F. Verstraete, Lieb-Robinson Bounds and the Generation of Correlations and Topological Quantum Order, Phys. Rev. Lett. **97**, 050401 (2006).

[42] M. B. Hastings, Locality in quantum systems, arXiv:1008.5137.

[43] P. Richerme, Z.-X. Gong, A. Lee, C. Senko, J. Smith, M. Foss-Feig, S. Michalakis, A. V. Gorshkov, and C. Monroe, Non-local propagation of correlations in quantum systems with long-range interactions, Nature (London) **511**, 198 (2014).

[44] T. Matsuta, T. Koma, and S. Nakamura, Improving the Lieb-Robinson bound for long-range interactions, Ann. Henri Poincare **18**, 519 (2017).

[45] M. Foss-Feig, Z.-X. Gong, C. W. Clark, and A. V. Gorshkov, Nearly Linear Light Cones in Long-Range Interacting Quantum Systems, Phys. Rev. Lett. **114**, 157201 (2015).

[46] M. C. Tran, A. Y. Guo, Y. Su, J. R. Garrison, Z. Eldredge, M. Foss-Feig, A. M. Childs, and A. V. Gorshkov, Locality and digital quantum simulation of power-law interactions, arXiv:1808.05225.

[47] H. J. Lipkin, N. Meshkov, and A. J. Glick, Validity of many-body approximation methods for a solvable model: (I). Exact solutions and perturbation theory, Nucl. Phys. **62**, 188 (1965).

[48] A. Sørensen and K. Mølmer, Entanglement and quantum computation with ions in thermal motion, Phys. Rev. A **62**, 022311 (2000).

[49] T. Monz, P. Schindler, J. T. Barreiro, M. Chwalla, D. Nigg, W. A. Coish, M. Harlander, W. Hänsel, M. Hennrich, and R. Blatt, 14-Qubit Entanglement: Creation and Coherence, Phys. Rev. Lett. **106**, 130506 (2011).

[50] A. del Campo, Shortcuts to Adiabaticity by Counterdiabatic Driving, Phys. Rev. Lett. **111**, 100502 (2013).

[51] S. Campbell, G. De Chiara, M. Paternostro, G. M. Palma, and R. Fazio, Shortcut to Adiabaticity in the Lipkin-Meshkov-Glick Model, Phys. Rev. Lett. **114**, 177206 (2015).

[52] S. Campbell and S. Deffner, Trade-Off Between Speed and Cost in Shortcuts to Adiabaticity, Phys. Rev. Lett. **118**, 100601 (2017).

[53] We note that the numerical optimization in our simulations may output local minima in the cost function, and thus the results presented in Fig. 2 are lower bounds on the optimal fidelities.

[54] D. Jaschke, K. Maeda, J. D. Whalen, M. L. Wall, and L. D. Carr, Critical phenomena and Kibble-Zurek scaling in the long-range quantum Ising chain, New J. Phys. **19**, 033032 (2017).

[55] S. Fey and K. P. Schmidt, Critical behavior of quantum magnets with long-range interactions in the thermodynamic limit, Phys. Rev. B **94**, 075156 (2016).

[56] T. Koffel, M. Lewenstein, and L. Tagliacozzo, Entanglement Entropy for the Long-Range Ising Chain in a Transverse Field, Phys. Rev. Lett. **109**, 267203 (2012).

[57] D. Vodola, L. Lepori, E. Ercolessi, and G. Pupillo, Long-range Ising and Kitaev models: Phases, correlations and edge modes, New J. Phys. **18**, 015001 (2016).

[58] C. Kokail, C. Maier, R. van Bijnen, T. Brydges, M. Joshi, P. Jurcevic, C. Muschik, P. Silvi, R. Blatt, C. Roos, and P. Zoller, Self-verifying variational quantum simulation of the lattice Schwinger model, Nature **569**, 355 (2019).

[59] A. Bapat and S. Jordan, Bang-bang control as a design principle for classical and quantum optimization algorithms, arXiv:1812.02746.